Journal of Engineering Mathematics, Vol. 4, No. 2, April 1970
Wolters-Noordhoff Publishing–Groningen
Printed in the Netherlands

Computation of Scattering from a Class of Bodies of Unrestricted Size

J. D. HUNTER AND R. H. T. BATES

Department of Electrical Engineering, University of Canterbury, Christchurch, New Zealand

(Received September 15, 1969)

SUMMARY

A method is presented for computing the scattering from any size of totally reflecting body by the inversion of one finite matrix, provided that the shape of the body can be derived by inwardly deforming a finite part of a body from which the scattering is known explicitly. Only the size of the deformed surface is limited by available computational facilities. The method, which is applicable to acoustic and electromagnetic scattering problems, is illustrated by applying it to a deformed infinite wedge for both electric polarization (Dirichlet problem: sound-soft boundary in acoustics), and magnetic polarization (Neumann problem: sound-hard boundary in acoustics). Numerical results are presented to demonstrate the convergence of the computations.

1. Introduction

Explicit solutions to scattering problems can be obtained for totally reflecting bodies having certain simple shapes [1], [2]. The geometrical theory of diffraction, derived from asymptotic forms of certain explicit solutions, can be used to predict approximately, but often with impressive accuracy, the field scattered from a wide class of bodies [3]. However, for dealing with penumbra and caustics the usefulness of the geometrical theory of diffraction is severely limited [4]. Also, because of the asymptotic nature of the theory, the separation between two diffracting vertices or edges on a body must be appreciable if the secondary diffracted field (the field diffracted from the second vertex or edge due to a ray diffracted from the first) is to be obtained accurately. Many writers [1], [4], [5], [6] have suggested improvements to the geometrical theory of diffraction for penumbra and caustics, but the asymptotic nature of the theory remains.

To be able to evaluate a suggested improvement to the geometrical theory of diffraction, accurate values should be available for the field scattered from bodies of basically simple shape, which have been deformed in many different ways. The computational procedure described here allows such accurate values to be obtained. The procedure is illustrated by applying it to a deformed wedge (Sections 4 and 5).

Using a digital computer, the field scattered from a body can be calculated using an integral equation over the body [7], [8], [9], [10]. The integral equation gives the scattered field as the radiation from sources induced in the surface of the body [11].

The discussion is now specialized to monochromatic electromagnetic scattering of angular frequency ω and wave number k. The time dependence $\exp(i\omega t)$ is suppressed in the analysis. When a perfectly conducting body having a surface σ is present in an incident field $\boldsymbol{U}_0$, the total field $\boldsymbol{U}$ surrounding the body is the sum of the incident and scattered fields. Thus, [8]

$$\boldsymbol{U} = \boldsymbol{U}_0 + \{\Lambda\} \int\!\!\int_\sigma \boldsymbol{g}(s)\Omega(\tau)ds\,, \quad \Omega(\tau) = \frac{\exp(-ik\tau)}{4\pi\tau}\,, \tag{1}$$

where τ is the distance from any point s on σ to the point at which $\boldsymbol{U}$ is observed and $\boldsymbol{g}(s)$ is the surface current density on σ, given by

$$\boldsymbol{g}(s) = \hat{\boldsymbol{n}} X \boldsymbol{H} \tag{2}$$

where $\hat{\boldsymbol{n}}$ is the outward unit normal vector at s. The vector operator $\{\Lambda\}$ is the scalar μ when $\boldsymbol{U}$

represents the vector potential $\boldsymbol{A}$, is $(-i\mu c^2(k^2+\nabla\nabla .)/\omega)$ when $\boldsymbol{U}$ represents the electric field $\boldsymbol{E}$, and is (∇X) when $\boldsymbol{U}$ represents the magnetic field $\boldsymbol{H}$. The symbols μ and c denote respectively the permeability of the medium and the velocity of electromagnetic waves. The wave number is assumed to have a vanishingly small, negative, imaginary part in order to ensure that the scattered field behaves in a physically acceptable manner at infinity.

Richmond [8] distinguishes between two approaches to solving (1); either the scattered field in a certain region, or the surface current density, may be expressed as a series of mode functions requiring the determination of unknown coefficients. These coefficients can be obtained by inverting a matrix derived from (1) and (2), and using the boundary conditions on σ. Since the matrix to be inverted must be finite, the moment method [12] chosen to represent the surface current density over the surface (usually the method of subsections) can only involve a finite number of mode functions. Because of this approximation to the surface current density, the scattered field given by (1) will not ensure that the total field is zero at all points in the interior of the body, and may, at certain frequencies, cause a resonant field to exist in the interior [9]. Therefore, it is important to note that even though the use of boundary conditions on the surface σ will suffice to give a close approximation to the scattered field using the method of moments, it is necessary to use the extended boundary conditions [9] to be certain of obtaining accurate values for the surface current density on σ.

The largest scattering body which can be dealt with by the method of moments is limited by the available computing facilities, since larger matrices are needed for larger bodies [7], [8], [12]. This paper introduces a technique, called the surface current replacement technique (Sections 2 and 3), based on the integral equation approach and using the extended boundary conditions, which enables the scattering from any size (even infinite) of perfectly conducting body to be determined by inversion of one finite matrix, provided that the shape of the body can be derived by inwardly deforming a finite part of a body from which the scattering is known explicitly. The technique involves expressing both the scattered field in a certain region, and the surface current density over the deformed part of the surface, in a series of mode functions with unknown coefficients. Hence, the size of only the deformed part of the surface is limited by available computing facilities. This technique is of the perturbation type, but solutions are obtained by the non-iterative procedure of inverting one finite matrix.

Although this paper deals explicitly with electromagnetic scattering, since the deformed wedge problems discussed in Sections 4 and 5 are two-dimensional, the results apply directly to acoustic scattering [13]. It is straightforward to transform the argument of Sections 2 and 3 into acoustic terms.

2. Surface Current Replacement Technique

The surface current replacement technique is based on the realization that any closed, perfectly conducting body with surface σ can be regarded electromagnetically as a region of zero field completely enclosed by radiating currents on σ. In the presence of an incident field, the function of these currents is to ensure that the total field internal to σ is zero at all points.

Consider a particular surface S in the presence of an incident field $\boldsymbol{U}_0$ (Fig. 1(b)). The closed surface S is separated into two open surfaces α and γ. Let surface currents be impressed on α so as to cancel exactly the surface currents already existing there. If γ is closed by a surface β to form a new closed surface S_1 (Fig. 1(a)) and the surface current density on S_1 is adjusted until there is zero field at all points inside S_1, then, electromagnetically, the total configuration is that of a perfectly conducting body with surface S_1 in the presence of the incident field $\boldsymbol{U}_0$. This argument is expressed analytically in Section 3.

If the field scattered from S, when it is illuminated by $\boldsymbol{U}_0$, is known then the surface current density of S is known. The problem of S_1 illuminated by $\boldsymbol{U}_0$ therefore resolves into the problem of S_1 illuminated by the field radiated by the known, impressed surface current distribution over α. The advantage of attempting to solve this latter problem, rather than the original of S_1 illuminated by $\boldsymbol{U}_0$, is that the sources of the incident field are now contained in a finite volume enclosing α. Thus, external to a volume enclosing α and β, the field may be written in an eigenfunction expansion with unknown coefficients, where each term in the expansion, besides satisfying the boundary conditions on γ, must represent an outward travelling wave in order to satisfy the radiation condition at infinity. This knowledge of the form of the field enables integrals over the surface γ to be evaluated analytically.

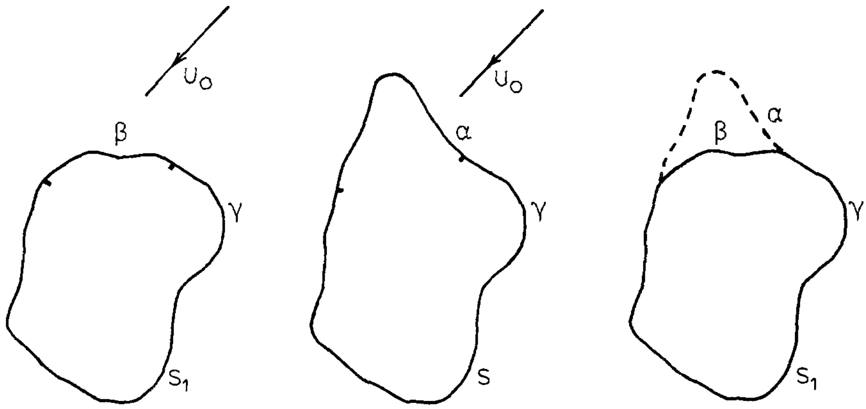

Figure 1. Deformation of surface S into surface S_1.

3. General Formulation

Consider a perfectly conducting closed body, having surface S_1, present in an incident field $\boldsymbol{U}_0$ (Fig. 1(a)). The total field $\boldsymbol{U}_1$ is given by [11]

$$\boldsymbol{U}_1 = \boldsymbol{U}_0 + \{\Lambda\} \iint_{S_1} \boldsymbol{h}(s)\,\Omega(\tau)\,ds\,, \tag{3}$$

where $\boldsymbol{h}(s)$ is the surface current density on S_1 and

$$S_1 = \beta \cup \gamma\,. \tag{4}$$

In order to evaluate $\boldsymbol{U}_1$ it is convenient first to treat two other problems:
(a) Consider a perfectly conducting, closed body with surface S, such that

$$S = \alpha \cup \gamma \tag{5}$$

illuminated by an incident field $\boldsymbol{U}_0$ (Fig. 1(b)). The total field $\boldsymbol{U}$ is given by

$$\boldsymbol{U} = \boldsymbol{U}_0 + \{\Lambda\} \iint_{S} \boldsymbol{i}(s)\,\Omega(\tau)\,ds\,, \tag{6}$$

where $\boldsymbol{i}(s)$ is the surface current density on S.
(b) Now consider S_1 illuminated by the field radiated by a surface current dentity $[-\boldsymbol{i}(s)]$ on α, which is external to S_1, as shown in Fig. 1(c). The total field $\boldsymbol{U}_2$ is given by

$$\boldsymbol{U}_2 = -\{\Lambda\} \iint_{\alpha} \boldsymbol{i}(s)\,\Omega(\tau)\,ds + \{\Lambda\} \iint_{S_1} \boldsymbol{f}(s)\,\Omega(\tau)\,ds \tag{7}$$

where $\boldsymbol{f}(s)$ is the surface current density on S_1.
Adding (6) and (7), and using (5), gives

$$\boldsymbol{U} + \boldsymbol{U}_2 = \boldsymbol{U}_0 + \{\Lambda\} \iint_{S_1} \boldsymbol{k}(s)\,\Omega(\tau)\,ds\,, \tag{8}$$

where the total surface current density $\boldsymbol{k}(s)$ on S_1 is given by

$$\begin{aligned} \boldsymbol{k}(s) &= \boldsymbol{f}(s) + \boldsymbol{i}(s)\,, \quad \text{on } \gamma\,, \\ &= \boldsymbol{f}(s)\,, \qquad\quad\;\; \text{on } \beta\,. \end{aligned} \tag{9}$$

From the argument of Section 2

$$U_1 = U_2 = 0, \text{ inside } S_1\,, \tag{10}$$

$$U = 0, \text{ inside } S\,. \tag{11}$$

Thus the problem represented by Fig. 1(a) is identical with the problem represented by the combination of Figs. 1(b) and 1(c). Hence,

$$U_1 = U + U_2 \tag{12}$$

and it follows from a comparison of (3) and (8) that

$$\boldsymbol{k}(s) \equiv \boldsymbol{h}(s)\,. \tag{13}$$

4. The Deformed Wedge

The surface current replacement technique is illustrated by applying it to calculating the scattering from an infinite wedge, the apex of which has been deformed (Fig. 2). The wedge is in a homogeneous isotropic medium and is illuminated by a plane wave which is normalized so that its magnetic field strength has unit magnitude. A detailed analysis is presented for electrically polarized fields (electric field parallel to z-axis, Dirichlet problem; sound-soft boundary in acoustics). Only the essential steps are noted for magnetically polarized fields (magnetic field parallel to z-axis; Neumann problem; sound-hard boundary in acoustics) since the analytical approach is similar to that used for electrically polarized fields.

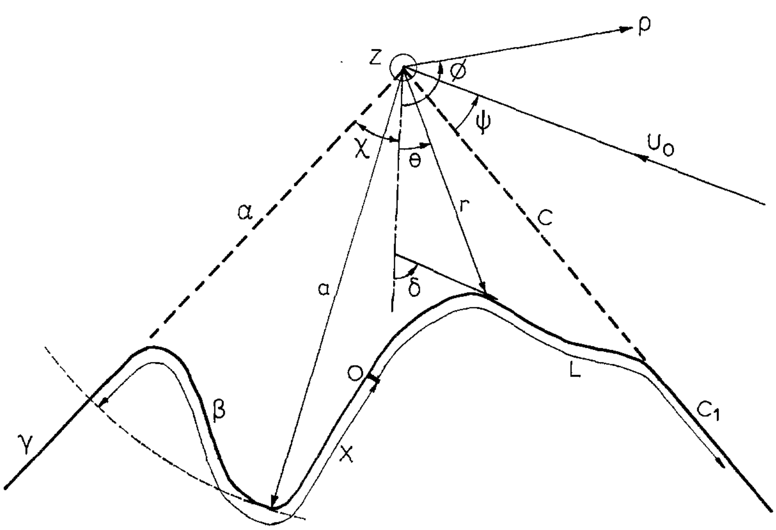

Figure 2. Deformed wedge. z-axis perpendicular to paper.

Since the problems considered in this section are two-dimensional there are no variations with z, so that the surface integrals in Sections 1 and 3 can be transformed into line integrals in the ρ, φ plane. Denote the geometrical cross-section of an arbitrary cylindrical body by Γ. The surface current density $\boldsymbol{g}(s)$ on the body is independent of z so that it is convenient to introduce the notation

$$\boldsymbol{g}(s) = \boldsymbol{G}(L) \tag{14}$$

where L denotes arc length along the periphery of the cross-section. Recognizing that τ, as defined in (1), can be written as $(R^2 + z^2)^{\frac{1}{2}}$, where R is the distance from any point on Γ to the point at which the field is observed, it follows that [1]

$$\iint_{\sigma} \boldsymbol{g}(s)\Omega(\tau)ds = \int_{\Gamma} \boldsymbol{G}(L)\int_{-\infty}^{\infty} \Omega(\tau)dz\,dL = \frac{-i}{4}\int_{\Gamma} \boldsymbol{G}(L)H_0^{(2)}(kR)dL \tag{15}$$

where $H_0^{(2)}(kR)$ is the Hankel function of the second kind of order zero.

The surface of the deformed wedge, denoted by C_1 in Fig. 2, and the first derivative of the surface in the direction of C_1, are taken to be continuous at all points on C_1.

Electric Polarization

Consider a perfectly conducting infinite wedge having cross-section C, occupying the region $|\varphi| \leqq \chi$, illuminated by an electrically polarized plane wave (Fig. 2). Use vector potential notation,

$$\mu \boldsymbol{H} = \nabla X \boldsymbol{A}, \quad \boldsymbol{A} = \hat{z}A \tag{16}$$

where $\hat{z}$ is the unit vector in the z-direction. The symbol U, which was used in Section 3, is replaced in this subsection by $\boldsymbol{A}$. The incident field is

$$A_0 = \frac{\mu}{k}\exp(ik\rho\cos(\varphi-\chi-\psi)). \tag{17}$$

The field surrounding C is [1]

$$A = \frac{4\mu\nu}{k}\sum_{n=1}^{\infty} i^{n\nu}J_{n\nu}(k\rho)\sin(n\nu[\varphi-\chi])\sin(n\nu\psi), \qquad \chi \leqq \varphi \leqq 2\pi-\chi, \tag{18}$$

$$\nu = \pi/2[\pi-\chi], \tag{19}$$

where $J_p(y)$ is the Bessel function of the first kind of argument y and order p.

All surface currents are directed parallel to $\hat{z}$. Using the notation introduced in (14), make the further definition

$$\boldsymbol{G}(L) = \hat{z}G(L). \tag{20}$$

For the undeformed wedge, define the apex to be the origin of L, with positive L on the right-hand side of the wedge. Using (2), (6), (14), (18) and (20) it follows that

$$I(L) = \frac{-4\nu}{kL}\sum_{n=1}^{\infty}(\operatorname{sgn}(L))^n n\nu i^{n\nu}J_{n\nu}(k|L|)\sin(n\nu\psi). \tag{21}$$

In Fig. 2 the cylindrical polar coordinates r and θ describe β which is the cross-section of the deformed part of the wedge. The maximum value of r is a. Thus, the sources of A_2 are contained within the circle $\rho=a$ and A_2 is entirely outgoing for $\rho>a$. A representation of A_2, which satisfies the radiation condition at infinity and the boundary conditions on the faces of the wedge, is then

$$A_2 = \frac{\mu}{k}\sum_{n=1}^{\infty} a_n H_{n\nu}^{(2)}(k\rho)\sin(n\nu[\varphi-\chi]), \quad \rho>a, \qquad \chi \leqq \varphi \leqq 2\pi-\chi, \tag{22}$$

where the coefficients a_n are yet to be determined.

Since the vector operator $\{A\}$ reduces in this subsection to μ, it follows from (7), (14), (15) and (20) that

$$A_2 = \frac{i\mu}{4}\int_{-a}^{a} I(L)H_0^{(2)}(kR)dL - \frac{i\mu}{4}\int_{C_1} F(L)H_0^{(2)}(kR)dL. \tag{23}$$

Denote the total arc length of β by $2X$. Denote by O that point on β which is distant X from both ends of β, when distance is measured along β. Define O to be the origin of L for the deformed wedge. A convenient, complete representation for $F(L)$ over β is

$$F(L) = \sum_{m=0}^{\infty} b_m J_m(kL), \qquad |L| < X, \tag{24}$$

where the coefficients b_m are yet to be determined. Note that (24) is consistent with the acknowledged behaviour of surface currents; that any oscillations exhibited by $F(L)$ are likely to have a spatial period close to the free-space wavelength [13].

The form of $F(L)$, on γ, is found from (22), using (2) and (16), to be

$$F(L) = \frac{-1}{k[|L|-X+a]} \sum_{n=1}^{\infty} a_n (\operatorname{sgn}(L))^{n+1} n\nu H_{n\nu}^{(2)}(k[|L|-X+a]), \qquad |L|>X\,. \tag{25}$$

The two representations (22) and (23), for A_2 can be equated on any circle $\rho=b$, provided that $b>a$. It is convenient to express A_2 as given by (23), in a trigonometrical Fourier series for the range $0 \leqq \varphi < 2\pi$. Thus,

$$A_2 = B_0^+ + 2 \sum_{p=1}^{\infty} [B_p^+ \cos(p\varphi) + B_p^- \sin(p\varphi)]\,, \qquad \rho=b\,, \tag{26}$$

where the $B_p^\pm$ are functions of b. Expanding (23), using Graf's addition theorem for Bessel functions [14], gives

$$\begin{aligned} B_p^\pm = -\frac{i\mu}{4}\Bigg[\Bigg[H_p^{(2)}(kb)\int_a^b [F(L+X-a) \pm F(-L-X+a)]\, J_p(kL)\,dL \\ + J_p(kb)\int_b^\infty [F(L+X-a) \pm F(-L-X+a)]\, H_p^{(2)}(kL)\,dL \\ - H_p^{(2)}(kb)\int_0^a [I(L) \pm I(-L)]\, J_p(kL)\,dL\Bigg] {\cos \atop \sin}(p\chi) \\ + H_p^{(2)}(kb)\int_{-X}^{X} F(L)\, J_p(kr) {\cos \atop \sin}(p\theta)\,dL\Bigg]. \end{aligned} \tag{27}$$

Since, from (10), A_2 is identically zero inside C_1 (that is for $|\varphi|<\chi$, $\rho>a$) it follows from (22) and (26) that

$$B_p^\pm = \frac{\mu\nu}{k\pi} {\cos \atop \sin}(p\chi) \sum_{n=1}^{\infty} \frac{t a_t H_{t\nu}^{(2)}(kb)}{(t\nu)^2-p^2}\,, \qquad t = {2n-1 \atop 2n}\,. \tag{28}$$

When (21) and (25) are substituted into (27), all the resulting integrals can be evaluated analytically [14]. When (27) and (28) are equated, all factors depending on b cancel out. On using (24) there results

$$\sum_{n=1}^{\infty} a_n D_{np} + \sum_{m=0}^{\infty} b_m C_{mp} = Y_p \tag{29}$$

where p is a non-negative integer, and

$$D_{np} = n\nu q_n(p\chi)\left[\frac{H_{n\nu}^{(2)}(ka)J_p(ka)}{n\nu+p} - ka\,\frac{H_{n\nu+1}^{(2)}(ka)J_p(ka) - H_{n\nu}^{(2)}(ka)J_{p+1}(ka)}{(n\nu)^2-p^2}\right], \tag{30}$$

$$C_{mp} = \frac{k}{2}\int_{-X}^{X} J_m(kL)\, J_p(kr)\, q_{m-1}(p\theta)\,dL\,, \tag{31}$$

$$Y_p = 4\nu^2 \sum_{n=1}^{\infty} q_n(p\chi)\, n i^{n\nu} \sin(n\nu\psi)\left[ka\,\frac{J_{n\nu+1}(ka)J_p(ka) - J_{n\nu}(ka)J_{p+1}(ka)}{(n\nu)^2-p^2} - \frac{J_{n\nu}(ka)J_p(ka)}{n\nu+p}\right], \tag{32}$$

$$q_{2n}(\varphi) = \sin(\varphi)\,, \quad q_{2n-1}(\varphi) = \cos(\varphi)\,. \tag{33}$$

To obtain numerical solutions, the two summations in (29) are truncated; the summation over n to N terms and the summation over m to M terms. In (29), the coefficients of a_n and b_m form a square matrix, of order $[N+M]$, which will be denoted by Δ. The series on the right-hand side of (32) is rapidly convergent so that the Y_p can be computed straightforwardly. Thus, the a_n and b_m are the elements of the column matrix $\Delta^{-1}Y$, where Y is the column matrix having Y_p for its elements. The accuracy with which a_n and b_m are obtained increases with $[N+M]$.

Since the surface C_1 of the deformed wedge and its first derivative in the direction of C_1 are continuous at all points on C_1, the edge conditions [1] indicate that the surface current density is continuous at all points on C_1. The right-hand sides of (21), (24) and (25) are absolutely continuous within their ranges of applicability so that $K(L)$, the total surface current density (refer to (9), (14) and (20)), is absolutely continuous everywhere on C_1 except at the junctions between β and γ. The continuity of $K(L)$ at $|L|=X$ is ensured by combining the equations

$$\sum_{n=1}^{\infty}(\pm 1)^{n+1}a_n\frac{n\nu}{ka}H_{n\nu}^{(2)}(ka)+\sum_{m=0}^{\infty}(\pm 1)^m b_m J_m(kX)=$$
$$-4\sum_{n=1}^{\infty}(\pm 1)^{n+1}\frac{\nu^2 n i^{n\nu}}{ka}J_{n\nu}(ka)\sin(n\nu\psi) \quad (34)$$

with (29). The elements of Δ are obtained from the left-hand side of (34) as well as the left-hand side of (29). Similarly, the elements of Y are obtained from the right-hand side of (34) as well as the right-hand side of (29).

The total field A_1 surrounding C_1 is the sum of A and A_2. When the a_n have been evaluated both A and A_2 are readily determined, from (18) and (22) respectively.

Magnetic Polarization

The symbol $\boldsymbol{U}$, which was used in Section 3, is replaced in this subsection by the magnetic field strength $\boldsymbol{H}$ where

$$\boldsymbol{H}=\hat{z}H. \quad (35)$$

The incident field is

$$H_0=\exp(ik\rho\cos(\varphi-\chi-\psi)), \quad (36)$$

and the field surrounding C is [1]

$$H=2\nu\sum_{n=0}^{\infty}\varepsilon_n i^{n\nu}J_{n\nu}(k\rho)\cos(n\nu[\varphi-\chi])\cos(n\nu\psi), \qquad \chi\leqq\varphi\leqq 2\pi-\chi, \quad (37)$$

where ε_n is the Neumann factor [14]. A suitable representation for H_2 is

$$H_2=\sum_{n=0}^{\infty}a_n H_{n\nu}^{(2)}(k\rho)\cos(n\nu[\varphi-\chi]), \qquad \rho>a, \qquad \chi\leqq\varphi\leqq 2\pi-\chi. \quad (38)$$

It is seen from (2) and (35) that all surface currents are directed perpendicular to $\hat{z}$. Using the notation introduced in (14), make the further definition

$$\boldsymbol{G}(L)=\hat{\boldsymbol{L}}G(L) \quad (39)$$

where $\hat{\boldsymbol{L}}$ is the unit vector, perpendicular to $\hat{z}$, tangent to the surface supporting the current and directed clockwise.

The analysis is similar to that for electric polarization. The vector operator $\{\Lambda\}$ has the form (∇X). It is again convenient to use the expression (24) for $F(L)$, for $|L| < X$. The coefficients a_n and b_m are found to satisfy

$$\sum_{n=0}^{\infty} a_n D_{np} + \sum_{m=0}^{\infty} b_m C_{mp} = Y_p\,, \tag{40}$$

where p is a non-negative integer, $D_{00} = i/v$ and

$$D_{np} = (-1)^{n+1} q_n(p\chi) p \left[\frac{H_{nv}^{(2)}(ka) J_p(ka)}{nv+p} - ka \frac{H_{nv+1}^{(2)}(ka) J_p(ka) - H_{nv}^{(2)}(ka) J_{p+1}(ka)}{(nv)^2 - p^2}\right], \tag{41}$$

$$C_{mp} = (-1)^m \frac{k}{4} \int_{-X}^{X} J_m(kL) \left[J_{p+1}(kr) q_m([p+1]\theta - \delta) + J_{p-1}(kr) q_m([p-1]\theta + \delta)\right] dL\,, \tag{42}$$

$$Y_p = 2vp \sum_{n=0}^{\infty} \varepsilon_n (-1)^n q_n(p\chi) i^{nv} \cos(nv\psi) \left[\frac{J_{nv}(ka) J_p(ka)}{nv+p} - ka \frac{J_{nv+1}(ka) J_p(ka) - J_{nv}(ka) J_{p+1}(ka)}{(nv)^2 - p^2}\right] \tag{43}$$

where the $q_n(\varphi)$ are defined in (33), and r, θ and δ are defined in Fig. 2. The continuity of $K(L)$ at $|L| = X$ is ensured by combining the equations

$$\sum_{n=0}^{\infty} (\pm 1)^n a_n H_{nv}^{(2)}(ka) - \sum_{m=0}^{\infty} (\pm 1)^m b_m J_m(kX) = -2v \sum_{n=0}^{\infty} (\pm 1)^n \varepsilon_n J_{nv}(ka) \cos(nv\psi) i^{nv} \tag{44}$$

with (40) when constructing the matrix Δ used for the evaluation of the a_n and b_m, which as before are the elements of the column matrix $\Delta^{-1} Y$.

5. Discussion of Computations for Deformed Wedge

The field scattered from any deformed wedge can be obtained from (29) and (41). The C_{mp} are the only quantities which have to be recalculated when the deformation is changed.

Notice that (29) and (41) are independent of b, the radius of the circle on which the two representations, (27) and (28), for the trigonometrical Fourier coefficients of the field are equated. Since the derivation of (27), and a similar but unquoted equation used in the analysis for magnetic polarization, is based on U_1 being identically zero for $\rho = b$, $|\varphi| < \chi$, it follows that (29) and (41) include the consequences of the extended boundary conditions. Analytic continuation arguments [9], [10] ensure that $U_1 \equiv 0$ everywhere inside C_1.

The a_n and b_m for certain round-topped wedges (circular deformation shown in Fig. 3) have been computed. It has been shown in Section 4 that the a_n and b_m can be obtained in general by inversion of a matrix of order $[N+M]$. However, the symmetry of the round-topped wedges permits the symmetric and anti-symmetric parts of the field to be separated on inspection. Consequently, the a_n and b_m can be obtained by the inversion of two matrices of approximate order $[N+M]/2$, which results in significant computational economy.

For the round-topped wedges the convergence of some coefficients is shown in Fig. 3. Since it is clear that convergence is occurring it can be deduced that the lower order modal components of U_2 predominate. Thus, accurate values for the surface current density can be obtained by truncating the summation on the right-hand side of (24).

Fig. 3 also illustrates the effect of including explicitly the continuity of the surface current density at the junctions between β and γ. The initial convergence of the a_n is seen to be more rapid.

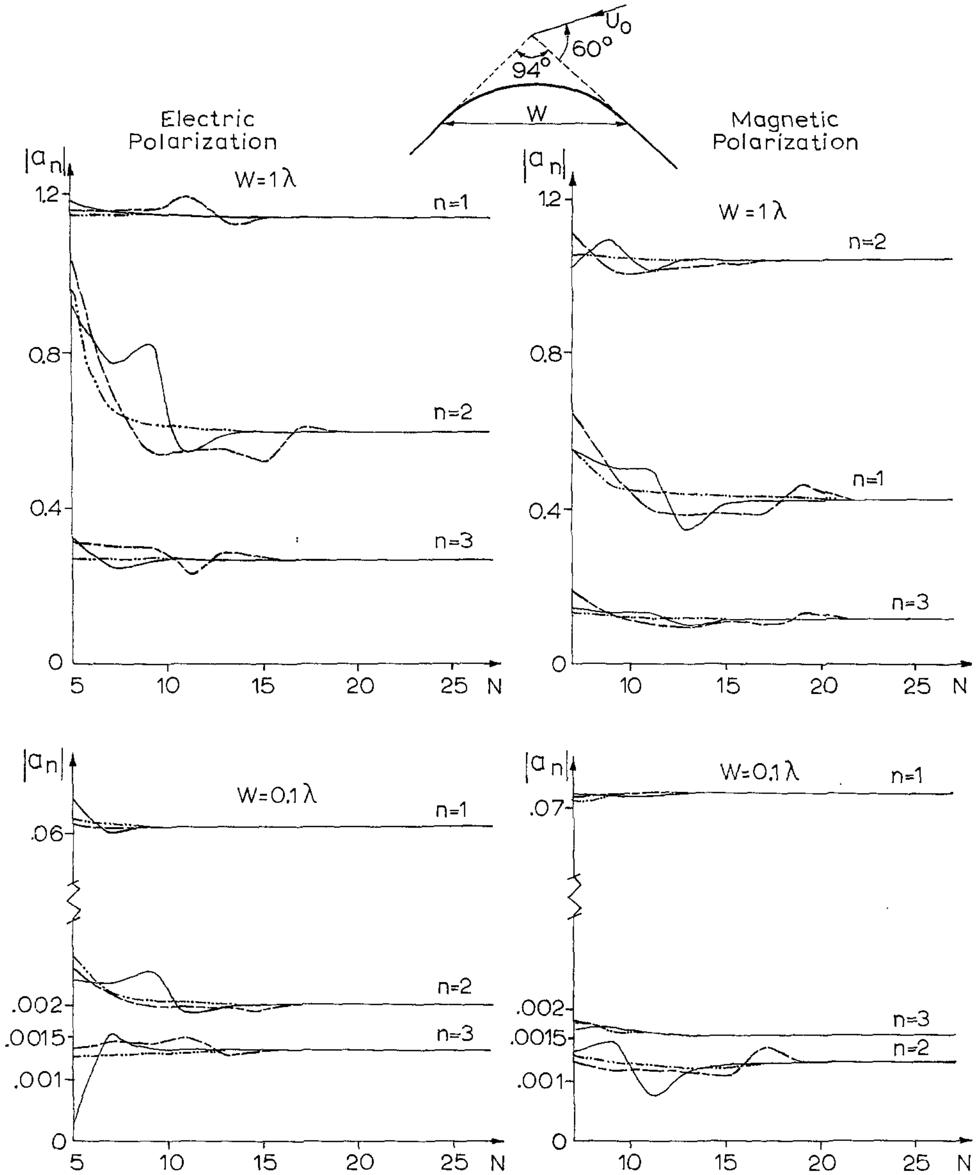

Figure 3. Convergence of the a_n field coefficients for the round-topped wedge. *Legend*: ——————— $M = 7$; ——— $M = 5$; —·—·— $M = 5$ and the continuity of the surface current density at the junctions of β and γ has been explicitly included.

In all the computations which have been done, the rate of convergence of the a_n and b_m (with n, m, N and M) indicates that accurate results are obtainable by inversion of finite matrices.

6. References

[1] D. S. Jones, *The Theory of Electromagnetism*, Pergamon, London, 1964.

[2] B. Noble, *Methods based on the Wiener-Hopf Technique for the Solution of Partial Differential Equations*, Pergamon, London, 1958.

[3] J. B. Keller, Geometrical Theory of Diffraction, *J. Opt. Soc. Amer.*, 52 (1962) 116–130.

[4] D. S. Ahluwalia, R. M. Lewis and J. Boersma, Uniform Asymptotic Theory of Diffraction by a Plane Screen, *SIAM J. Appl. Math.*, 16 (1968) 783–807.

[5] J. S. Yu and R. C. Rudduck, On Higher Order Diffraction Concepts Applied to a Conducting Strip, *IEEE Trans. Ant. and Proc.*, AP-15 (1967) 662–668.

[6] M. A. K. Hamid, Near Field of a Conducting Wedge, *IEEE Trans. Ant. and Prop.* (Commun.), AP-15 (1967) 490–492.

[7] M. G. Andreasen, Scattering from Parallel Metallic Cylinders with Arbitrary Cross Sections, *IEEE Trans. Ant. and Prop.*, AP-12, (1964) 746–754.
[8] J. H. Richmond, Digital Computer Solutions of the Rigorous Equations for Scattering Problems, *Proc. IEEE,* 53 (1965) 796–804.
[9] P. C. Waterman, Matrix Formulation of Electromagnetic Scattering, *Proc. IEEE,* 53 (1965) 805–812.
[10] R. H. T. Bates, Modal Expansions for Electromagnetic Scattering from Perfectly Conducting Cylinders of Arbitrary Cross-Section, *Proc. IEE,* 115 (1968) 1443–1445.
[11] H. Hönl, A. W. Maue and K. Westpfahl, *Handbuch der Physik,* 25, Berlin, Springer-Verlag, (1961), 240.
[12] R. F. Harrington, *Field Computation by Moment Methods,* Macmillan, New York, 1968.
[13] C. J. Bouwkamp, Diffraction Theory, *Rpts. Prog. Phys.*, XVII (1954) 35.
[14] G. N. Watson, *A Treatise on the Theory of Bessel Functions,* Cambridge Univ. Press, 1944.

Journal of Engineering Math., Vol. 4 (1970) 119–128